

Peak Acceleration of Horizontal and Vertical Components for Near-Field Earthquake Motions

Makoto Watabe

University of Tokyo Metropolitan, Tokyo, Japan

Masanobu Tohdo

Toda Construction Co., Tokyo, Japan

Nikolaos A. Theofanopoulos

University of Tokyo Metropolitan, Tokyo, Japan

INTRODUCTION

It is well known that active faults can be found anywhere in Japan. Considering that fact in seismic design of structures, it is essential to evaluate the intensities of earthquake ground motions (EGMs), e.g. peak accelerations, at short distances from fault. Especially for the seismic design of nuclear power plants in Japan (level S2), it is officially required to assume that an earthquake with magnitude of 6.5 occur close to the plant site. It has been observed from various records that the attenuation law for peak acceleration in the near-field is not similar to that in the far-field. Moreover, the graph of the peak acceleration versus the distance to the fault seems to be flat for short distances to the fault, phenomenon that is called saturation of peak acceleration. Taking into account that phenomenon, various formulae to predict peak acceleration have been proposed (Refs.6-8). However, the number of earthquakes in which EGMs near faults had been recorded is limited, therefore the prediction by the above formulae may not be adequate. From this point of view, it seems to be necessary that the prediction should be complemented by another approach.

Up to the present, various methods accounting the fault model to synthesize EGMs have been proposed (e.g. Refs.1-3). In the first part of this paper for the evaluation of near-field strong EGMs, is presented a method, in which EGMs due to a large event are synthesized by superposing elementary waves radiated from each subfault taking into account the time lag for the fault rupture and wave propagation. Our method uses an empirical formula for the velocity response spectra in terms of magnitude and distance to set the amplitude spectra of the elementary waves.

Many accelerograms in the near-fault region have been observed in USA. Based on these data, the relationship between peak acceleration of vertical and horizontal components is discussed in the second part of this paper.

SYNTHESIS OF NEAR-FIELD EARTHQUAKE MOTIONS BY FAULT MODEL

Superposition Procedure

In the synthesis, the fault plane of a large earthquake with magnitude M is divided into small $N \times N$ sub-faults as shown in Fig.1 which correspond to smaller events with magnitude m . The fault length (L) and the width (W) can be estimated by Eq.(1) (Ref.4).

$$\log L \text{ (in km)} = 0.5 \cdot M - 1.88, \quad W = L/2 \quad (1)$$

The scaling factor between the large and small event was assumed as

$$L/Le = W/We = N = 10^{0.5*(M-Me)} \quad (2)$$

The synthesis of an acceleration EGM $U(t)$ at an observatory is accomplished by superposing elementary waves radiated from each subfault expressed as

$$U(t) = \sum_{i=1}^N \sum_{j=1}^N \sum_{k=1}^{NK(T)} U_{eijk} \{t - \text{trij} - (k-1) \cdot \text{Tre} - r_{ij}/V_s\} \quad (3)$$

Where trij is the start time of rupture of the element (i, j) , V_s the shear wave velocity of wave propagation, r_{ij} is shown in Fig.1 and Tre is the rise-up time given by Eq.(4).

$$\log \text{Tre (in sec.)} = 0.5 \cdot M_e - 3.03 \quad (4)$$

The $NK(T)$ for summation with respect to k in Eq.(3) is assumed to be period dependent and is defined by Eq.(5).

$$\log NK(T)/N = -(M-Me) \cdot 0.6 \cdot \exp(-3T), \quad T; \text{sec.} \quad (5)$$

The elementary wave is represented by Eq.(6) as nonstationary random process multiplied by envelope function $E(t)$ with duration time of t_{de} .

$$U_{eijk}(t) = E(t) \cdot U_{sijk}(t) \quad (6)$$

$$E(t) = t/t_m \cdot \exp(1-t/t_m), \quad t_m = l_e/(2 \cdot v_r) + \text{Tre} \quad (7)$$

Where l_e is the length of the subfault in the direction of rupture and v_r is the fault rupture velocity. The stationary process is generated as follows.

$$U_{sijk}(t) = \sum_T 2/t_{de} \cdot F_{sij}(T) \cdot \cos(2\pi/T \cdot t + \phi) \quad (8)$$

$$F_{sij}(T) = S_{vo}(M_e, r_{eij}, T) / \sqrt{PE}, \quad PE = (e/2)^2 \cdot t_m / t_{de} \quad (9)$$

$S_{vo}(T)$ in Eq.(9) is obtained by substituting M_e and r_{eij} into Eq.(10).

$$\begin{aligned} \log S_{vo}(M=M_e, X=r_{eij}, T) &= 0.607 \cdot M - 1.19 \cdot \log X - 0.85 \\ &+ a_1 \cdot \{1 - (T/a_2)^{a_3}\} \cdot \{1 + T \cdot \exp(1 - a_4 \cdot T)\} - 0.25 \cdot X^{0.1} \cdot (1/\sqrt{T} - 1) \\ ; a_1 &= 0.015 / (M/8)^{14} + 0.055, \quad a_2 = 0.045 \cdot 1.6^M, \\ a_3 &= 1.8 \cdot (M/8)^{13} / \{(M/8)^{13} + 0.15\}, \quad a_4 = 0.1 / (M/8)^{15} + 0.9 \end{aligned} \quad (10)$$

Where $S_{vo}(T)$ expressed by Eq.(10) is the zero damping velocity response spectrum proposed by the authors based on the analyses of observed accelerograms on rock sites having shear wave velocity between 0.6 and 1.0 km/sec (Ref.5). Considering the fact that in the near-field region even in the case of a fault with small dimensions the tendency of saturation of peak acceleration exists, the equivalent distance r_{eij} to determine the amplitude spectra in Eq.(8) was defined as follows.

$$r_{eij} = \left[\int_0^{Le} \int_0^{We} \{r_m + r(x, y)\}^{-2.5} dx dy / (LeWe) \right]^{-1/2.5}, \quad r_m = 0.75 \sqrt{LeWe/\pi} \quad (11)$$

In the synthesis of Eq.(3), the phase angles ϕ in Eq.(8) were generated by random number. Consequently, the elementary waves were uncorrelated each other in terms of i, j and k . In the latter parts, we assumed $v_r = 3 \text{ km/s}$, $V_s = 3.5 \text{ km/s}$ and uni-lateral rupture of fault. N was estimated by Eq.(2) assuming that the magnitude M_e of the small event is about 5.5.

Parametric Studies

Using the method presented above, parametric studies on peak acceleration and velocity values were carried out, changing the magnitude M , closest distance to fault (dc) and direction (θ) as shown in Fig.2. Examples of synthetic wave form for $M=6.5$ ($N=4$) are traced in Fig.3. The relationships between dc and peak

acceleration (A) or peak velocity (V) are plotted in Figs.4 and 5, respectively. On the basis of these studies it was found that the empirical formulae to evaluate the peak values in the near-field can be expressed as follows.

$$\begin{aligned} \log A \text{ (in Gal)} &= 0.440*M-1.38*\log XA+1.04 \\ \log V \text{ (in cm/s)} &= 0.607*M-1.19*\log XV-1.40 \end{aligned} \quad (12)$$

Where XA and XV (in km) are given by

$$\begin{aligned} XA &= \{ (dc+0.6*L^{0.5})^2 + (1.4*L^{0.5})^2 \}^{1/2} \\ XV &= \{ (dc+0.4*L^{0.6})^2 + (L^{0.6})^2 \}^{1/2} \end{aligned} \quad (13)$$

The solid lines in Figs.4 and 5 are estimated by Eqs.(12). Figures 6 and 7 show comparisons among Eqs.(12) and other estimations by Refs.6, 7 and 8 along with the plots estimated by tombstone behavior at rock in earthquakes (Ref.9). In the plot due to Ref.7, peak accelerations are divided by 1.13. It should be noted here that in the statistical analyses by Joyner et al. and Campbell the data observed at soil sites had been included.

PEAK ACCELERATION OF VERTICAL EARTHQUAKE MOTIONS RECORDED IN USA

In order to examine the relationship between the peak acceleration of vertical and horizontal components, 61 records (3 components in each record) due to 11 earthquakes in USA shown in Table 1 were used. The relationship between moment magnitude and fault distance of these records is shown in Fig.8. The peak acceleration (Av) of vertical components versus distance is plotted in Fig.9. From this figure it can be recognized that the Av of EGMs observed at the sites close to the fault during the 1979 Imperial Valley Earthquake or at Gilroy Array during the Morgan Hill Earthquake are considerable larger than the average values due to other records with the magnitude of approximately the same level at the same distances.

As an example of such accelerograms, three components of EGMs observed at No.6 site of El-Centro Array during the 1979 Imperial Valley Earthquake are traced in Fig.10. It can be observed that in the vertical component a spike of very high peak acceleration appears at the early time of time history. The use of such Av in statistical analysis may not be adequate, because such sharp peak values may be owed to irregular rupture of the fault or to the high soil amplification. From this point of view, we used the peak acceleration (Avs) of vertical component occurring during the strong part of time history of horizontal components as shown by the dashed line in Fig.10. The peak value of horizontal components is represented by the geometrical mean (Ah) of peak values of the two horizontal components.

The relationship between Avs and Ah is plotted in Fig.11. The distribution of the ratio of Avs/Ah for the data base is illustrated in Fig.12. The geometrical mean of Avs/Ah was equal to 0.53. Using this result we can estimate the peak acceleration (Avs) of vertical component. The estimation is performed by multiplying the Ah due to the formula proposed by Joyner et al. (Ref.7) by 0.53/1.13. The results are shown by the dashed lines in Fig.13 along with the plots of Avs of observed EGMs. The Av estimated by the formula proposed by the authors (Ref.5) is additionally drawn by the solid lines in Fig.13. In Fig.14, the distribution of the ratio of observed Avs to estimated one, i.e. estimation error, is illustrated.

CONCLUSIONS

In the first part, a method to synthesize near-field earthquake ground motions has been presented. Based upon this method, parametric studies have been performed and relationships to estimate the peak acceleration of horizontal components have been proposed. From these results it was found that the peak

acceleration of horizontal component at rock sites just close to the fault due to earthquakes with magnitude between 6.5 and 7.5 became 500 to 600 Gals.

In the second part, correlations between the peak acceleration of vertical and horizontal components observed in USA have been established. The mean ratio of the peak acceleration of vertical and horizontal components was equal to 0.53. Then, it was verified that it is possible to estimate satisfactorily the peak acceleration of vertical components by multiplying the results given by the relationships proposed by Joyner et al. by 0.53.

REFERENCES

1. Harzell, S., "Earthquake Aftershocks as Green's Functions," Geophys. Res. Letters, 5, 1-4, (1978).
2. Irikura, K., "Semi-Empirical Estimation of Strong Ground Motions During Large Earthquakes," Bull. Disas. Prev. Res. Inst., Kyoto Univ., 33, 63-104, (1983).
3. Tohdo, M. and Watabe, M., "Evaluation of Intensities of Near-Field Earthquake Ground Motions by Using the Empirical Formula for Velocity Response Spectra," 9th WCEE, (1988)
4. Sato, R., "Theoretical Basis on Relationships between Focal Parameters and Earthquake Magnitude," J. Phys. Earth., 27, 353-372, (1989).
5. Ohsaki, Y., Watabe, M. and Tohdo, M., "Analyses on Seismic Ground Motion Parameters," 7th WCEE, 2, 97-104, (1980).
6. Kanai, K. and Suzuki, T., "Expectancy of the Maximum Velocity Amplitude of Earthquake motions at Bedrock," Earthq. Res. Inst., Univ. of Tokyo, XLVI, (1968).
7. Joyner, W.B. and Boore, D.M., "Peak Horizontal Acceleration and Velocity from Strong Motion Records Including Records from the 1979 Imperial Valley, California, Earthquake," Bull. Seism. Soc. Am., 71, 2011-2038, (1981).
8. Campbell, K.W., "Near-Source Attenuation of Peak Horizontal Acceleration," Bull. Seism. Soc. Am., 71, 2039-2070, (1981).
9. Omote, S., Miyake, A. and Narahashi, H., "On Maximum Accelerations in Near-Field (in Japanese)," Annual Meeting of A.I.J., 549-550, (1978).

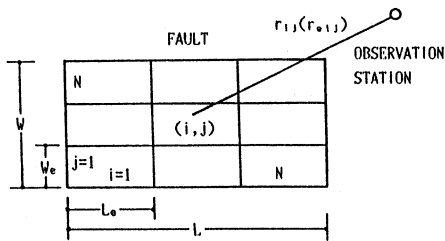


Fig.1 Schematic Views of Main Fault and Subfaults and Observatory for Synthesis

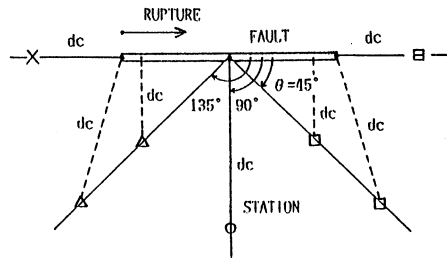


Fig.2 Geometries for Parametric Studies

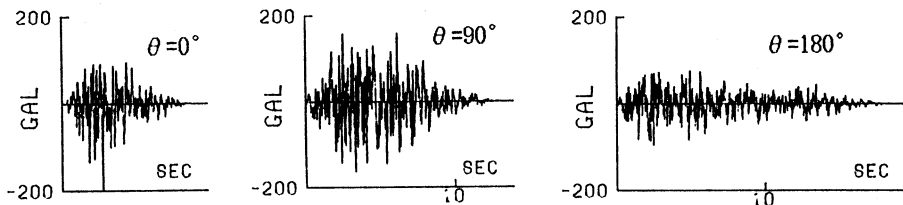


Fig.3 Synthesized Time Histories (M=6.5, dc=12km)

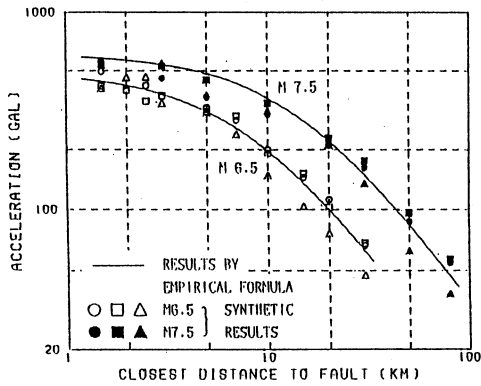


Fig.4 Peak Acceleration versus d_c obtained by Synthesis and Eq.(12)

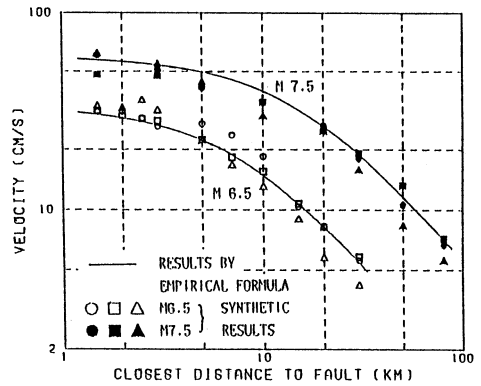


Fig.5 Peak Velocity versus d_c obtained by Synthesis and Eq.(12)

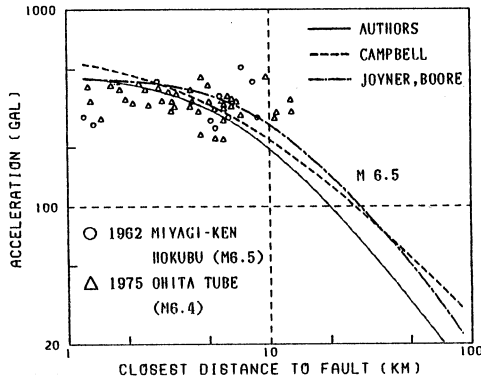


Fig.6 Comparison of Peak Acceleration estimated by the Authors and Others (M=6.5)

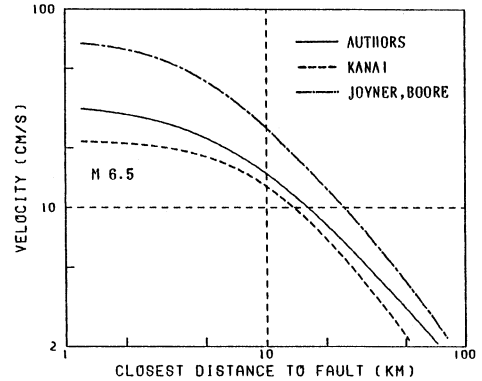


Fig.7 Comparison of Peak Velocity estimated by the Authors and Others (M=6.5)

Table 1 Earthquakes of the Data Base recorded in USA

EARTHQUAKE	DATE	DEPTH (KM)	MAGNITUDE		FAULT TYPE	MARK
			M_w	M_L		
IMPERIAL VALLEY	1940 5/18	18.0	7.0	6.4	STRIKE	○
KERN COUNTY	1952 7/21	18.0	7.4	7.2	STRIKE	△
SAN FRANCISCO	1957 3/22		5.3	5.3	STRIKE	□
PARKFIELD	1966 6/27	6.0	6.1	5.5	STRIKE	×
BORREGO Mtn	1968 4/ 8	11.1	6.6	6.7	STRIKE	×
LYTLE CREEK	1970 9/12	8.0	5.3	5.4	STRIKE	⊖
SAN FERNANDO	1971 2/ 9	13.0	6.6	6.4	REVERSE	△
HOLLISTER	1974 11/28	9.0	5.2	5.2	STRIKE	⊞
COYOTE LAKE	1979 8/ 6	9.6	5.8	5.9	STRIKE	×
IMPERIAL VALLEY	1979 10/15	12.0	6.5	6.6	STRIKE	●
MORGAN HILL	1984 4/24	9.0	6.2	6.2	STRIKE	×

M_w ; MOMENT MAGNITUDE , M_L ; LOCAL MAGNITUDE

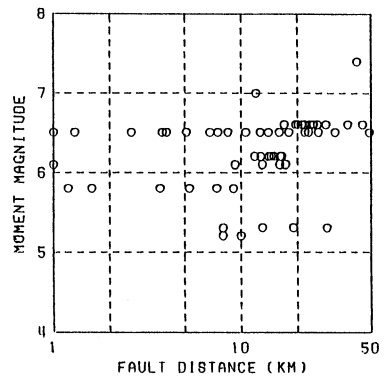


Fig.8 Relationship between Moment Magnitude and Fault Distance of the Data Base

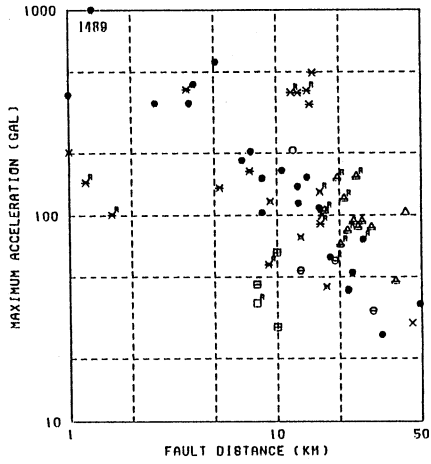


Fig.9 Vertical Peak Acceleration versus Fault Distance of the Data Base

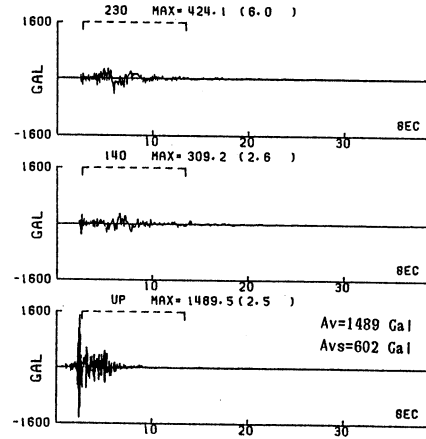


Fig.10 Time Histories observed at No.6 Site during the 1979 Imperial Valley Earthquake

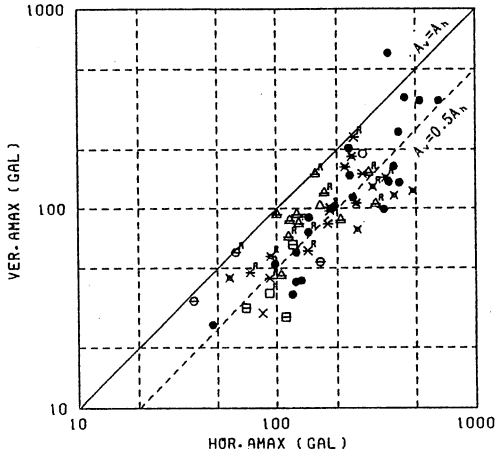


Fig.11 Relationship between Peak Acceleration (A_v s) of Vertical Component except "Spike" and That (A_h) of Horizontal Component

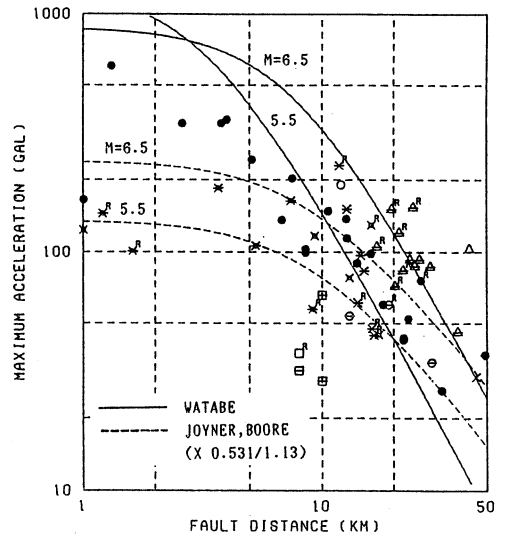


Fig.13 Comparison of observed A_v s and estimated Ones

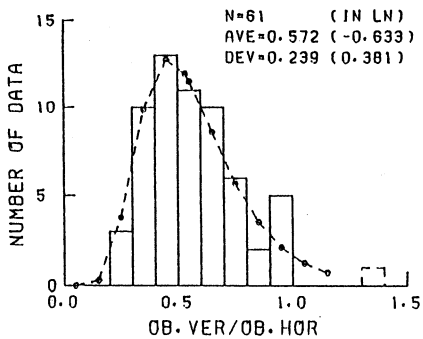


Fig.12 Distribution of A_v/A_h
(The mean value is equal to 0.53.)

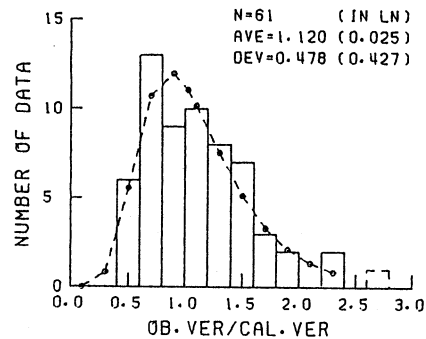


Fig.14 Distribution of the Ratio of observed A_v s to estimated One by multiplying the Result given by Joyner et al. by 0.53